View metadata, citation and similar papers at core.ac.uk

brought to you by CORE

provided by Elsevier - Publisher Connector

Available online at www.sciencedirect.com

ScienceDirect

Physics Procedia 76 (2015) 42 – 46

Physics Procedia

The 17th International Conference on Luminescence and Optical Spectroscopy of Condensed Matter (ICL2014)

Photo-generated Carrier Dynamics of InGaN/GaN Nanocolumns

Naoki Shimosako[a], Yuta Inose[a], Kazuhiro Ema[a,b], Yusuke Igawa[a] and Katsumi Kishino[a,b].

[a]*Sophia University, 7-1 Chiyoda-Ku, Tokyo 102-8554, Japan*
[b]*Sophia Nanotechnology Research Center, Sophia University, 7-1 Chiyoda-Ku, Tokyo 102-8554, Japan*

Abstract

We have investigated the photon-generated carrier dynamics of InGaN/GaN nanocolumns whose emission wavelength is in the orange to red region, focusing on the changes in the photoluminescence spectra, emission efficiency and relaxation curves. We have explained these changes by considering the filling of non-radiative centers, emission from localized states, the processes above the mobility-edge density and other non-radiative processes.

© 2015 The Authors. Published by Elsevier B.V. This is an open access article under the CC BY-NC-ND license (http://creativecommons.org/licenses/by-nc-nd/4.0/).
Peer-review under responsibility of The Organizing Committee of the 17th International Conference on Luminescence and Optical Spectroscopy of Condensed Matter

Keywords: InGaN, nanoscolumns, photoluminescence

1. Introduction

$In_xGa_{1-x}N$ has attracted increasing interest for light emitting devices since its band gap energy varies from 3.5 eV (ultraviolet) to 0.65 eV (infrared) by changing the composition ratio x. However, the emission efficiency of InGaN thin films rapidly decreases on increasing the composition ratio x because of increasing threading dislocations and internal electric fields. Nanocolumn crystals have a great potential to solve this problem. A nanocolumn is a columnar crystal, whose diameter is about 100 nm and height is about 1 μm [1]. They exhibit a strong photoluminescence (PL), even in the yellow to red region, because of the relaxation of internal electric fields and a reduction of threading dislocations [2]. Sekiguchi *et al.* have succeeded to control the emission wavelength of InGaN nanocolumns by changing the diameter of the columns [3]. The use of nanocolumns is very likely to accelerate the development of red and yellow semiconductor lasers. However, the basic photo-excited carriers property of nanocolumns have not been fully clarified, although a full understanding of the carrier dynamics is necessary for such applications.

1875-3892 © 2015 The Authors. Published by Elsevier B.V. This is an open access article under the CC BY-NC-ND license (http://creativecommons.org/licenses/by-nc-nd/4.0/).
Peer-review under responsibility of The Organizing Committee of the 17th International Conference on Luminescence and Optical Spectroscopy of Condensed Matter
doi:10.1016/j.phpro.2015.10.008

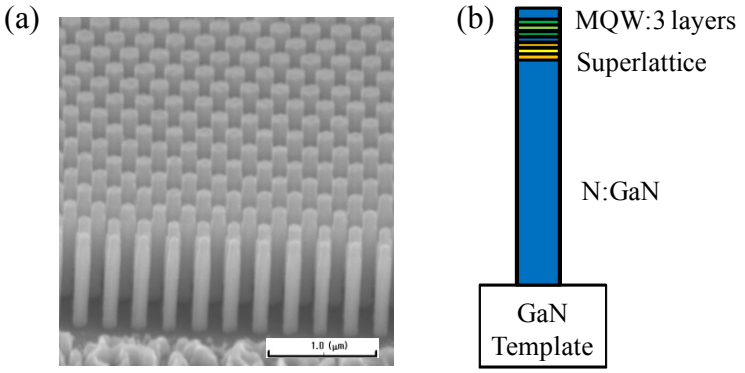

Fig. 1 (a) A SEM image of the nanocolumn sample. (b) Schematic of nanocolumn structure.

In this study, we focus on the photo-excited carrier dynamics of InGaN/GaN multiple quantum well nanocolumns whose wavelength is in the orange-to-red region. We have measured time integral PL and time-resolved PL (TRPL) spectra over a wide excitation range, and analyzed the excited-carrier density dependence of the spectral shape, the PL efficiency and decay time to obtain insights into the photo-excited carrier dynamics.

2. Experiment

We used two samples; one having InGaN/GaN nanocolumns and a thin film for reference. The nanocolumn sample was grown by molecular beam epitaxy [4], and the diameter was 150 nm and the column interval was 200 nm. Figure 1(a) shows a bird's-eye view scanning electron microscopy (SEM) image. The nanocolumn has InGaN/GaN multiple quantum wells (MQWs) which consist of three periods of InGaN wells with 6 nm thickness and barriers of 18 nm GaN as schematically shown in Fig. 1(b). The emission wavelength of the nanocolumn sample is in the orange-to-red region (see Fig. 2).

The film sample was grown by metal-organic vapor phase epitaxy. The film has also MQWs which consist of three periods of InGaN wells with 3 nm thickness and barriers of 12 nm GaN. Since the quality of film samples generally deteriorates in the longer-wavelength region rather than in the green region, we cannot prepare a film sample having the same emission wavelength as that of the nanocolumn sample. The film sample we used has 2.3 ~ 2.5 eV emission wavelength (green region).

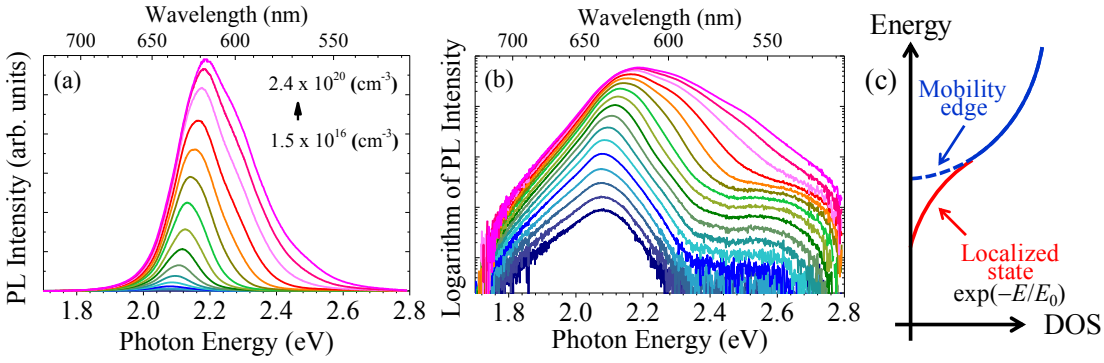

Fig. 2 The carrier density dependence of PL spectra of nanocolumns on linear (a) and logarithmic (b) scales. (c) Schematic of density of states (DOS) for localized states.

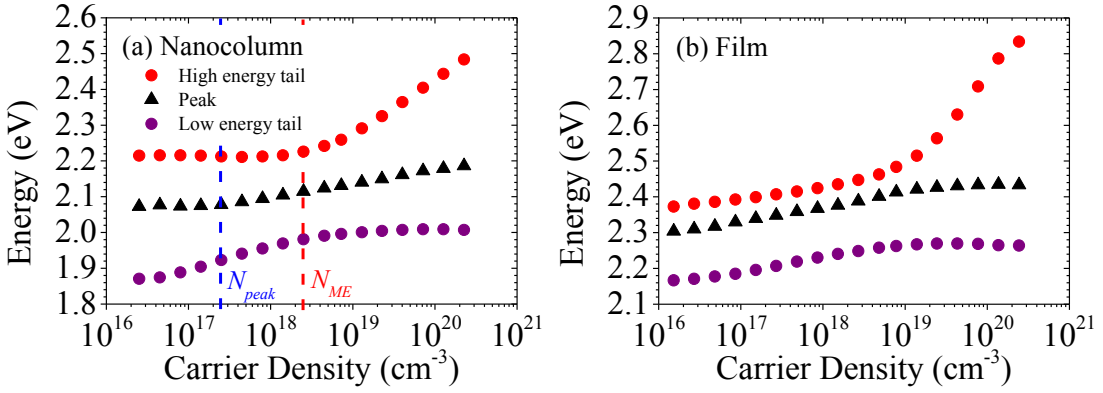

Fig. 3 Carrier density dependence of the peak energy, high energy tail and low energy tail ($1/e^2$ x peak) of the nanocolumn and film samples.

We measured the photo-excited carrier density dependence of the PL spectra and TRPL decay curves at liquid nitrogen temperature. These measurements were performed using a micro-spectroscopy technique with a spatial resolution of 0.7 μm. TRPL measurements were carried out with a 400 nm femtosecond pulsed laser for the excitation and a streak camera with a time resolution of about 180 ps.

3. Result and discussion

Figure 2(a) and (b) show the carrier density dependence of the PL spectra of the nanocolumn sample on linear and logarithmic scales, respectively. We can see that the spectrum becomes broad with increasing the carrier density, particularly on the high-energy side. On the other hand, the low-energy region of the spectrum does not show strong broadening, and the low-energy tail shapes at higher densities ($N > 2.5 \times 10^{18}$ cm^{-3}) show a constant gradient on the logarithmic scale, indicating that the low energy region of the PL spectrum has an exponential tail. The value of the gradient at room temperature was the same as that at liquid nitrogen temperature. We can conclude that the low-energy exponential tail of the PL spectrum reflects the density of states (DOS) of the localized states, as shown in Fig. 2(c). It is known that InGaN has such localized states below the band gap due to indium composition fluctuations. Since the localized states are filled up randomly from deep energy states, the emission from the deep states (i.e. low-energy tail of the spectrum) reflects the DOS of the localized states at sufficiently high carrier concentrations. The tailing parameter E_0 estimated from the gradient is about 50 meV.

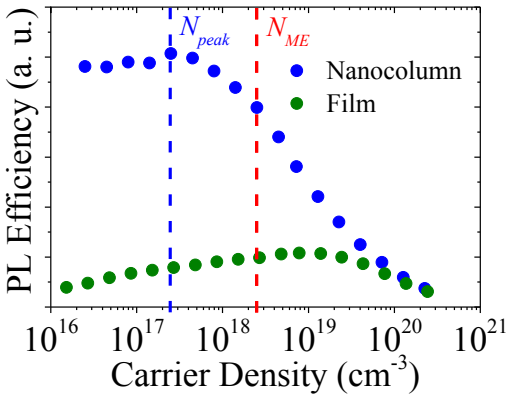

Fig. 4 PL efficiency of the film and nanocolumn samples.

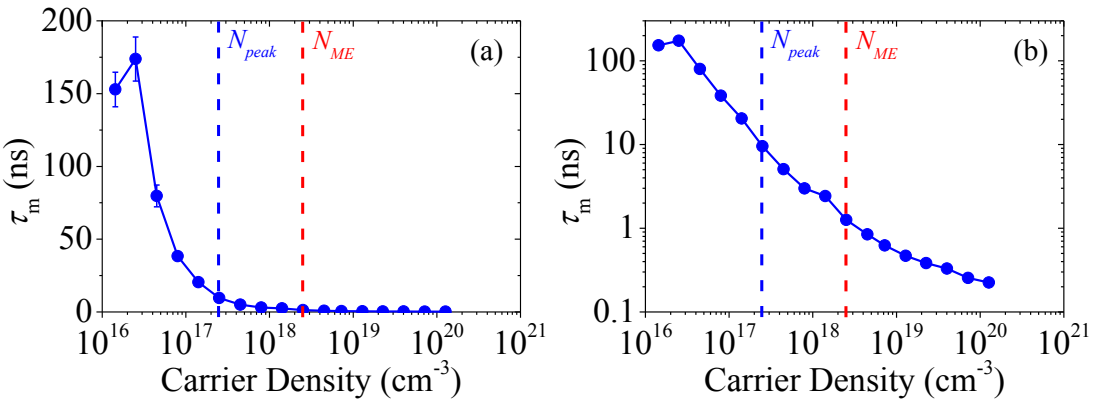

Fig. 5 The average relaxation time τ_m on linear (a) and logarithmic (b) scales.

In order to analyze the blue shift and the broadening in detail, we plotted the peak energy, high energy tail and low energy tail, which are defined by the energy position at $1/e^2$ of the peak intensity, as a function of the carrier density. Figure 3(a) shows the result, where the same plots for the film sample are also shown in (b). We can see that above a certain carrier density (denoted by "N_{ME}"), the high energy tail shows a strong blue shift and thus the spectrum shows a distinct broadening. This means that the excited carrier density exceeds the mobility edge (see Fig.2 (c)) above N_{ME}. From the position of N_{ME} in Fig. 3 we can estimate the densities of the localized states for the nanocolumns and film samples to be ~ 2 x 10^{18} cm^{-3} and ~ 10^{19} cm^{-3}, respectively. Below N_{ME} the behaviour of these plots are different between the nanocolumn and the film samples. For the film, the peak and both tails show blue shifts, while the high energy tail shows no blue shift for the nanocolumn. This discrepancy may arise from the fact that the film has a large internal electric field, but the nanocolumns have no or little internal electric field.

Figure 4 shows the PL efficiency of the both samples. The nanocolumn sample shows higher efficiency than the film although the PL from the nanocolumns is in the orange to red region. The PL efficiency of the column sample reaches a maximum at the carrier density N_{peak}.

In the analysis of the TRPL measurements, we fitted each TRPL with a stretched exponential function $I(t) = I_0 \exp[-(t/\tau_0)^{\beta}]$ [5][6]. Such a stretched exponential function is effective for the TRPL of InGaN because InGaN has various energy level emissions with different relaxation times [7][8]. The parameter β represents the distribution of carrier relaxation times. As β ($0 < \beta \leq 1$) approaches 0, the relaxation time has a wider distribution. We can obtain the parameters β and τ_0 by fitting the TRPL data. It should be noted that τ_0 does not mean a characteristic time constant of the distributed time constants. We have to deduce the average relaxation time τ_m from the calculation using the parameters β and τ_0 [7]. Figure 5(a) and (b) show the carrier density dependence of obtained τ_m on linear and logarithmic scales, respectively.

At very low carrier density (~ 10^{16} cm^{-3}), τ_m increases because the carriers fill up non-radiative centers, i.e. the disappearance of the path to the non-radiative decay increases the total PL decay time. After the non-radiative centers are filled up, τ_m decreases monotonically. This is a characteristic behaviour of emissions from localized states. If both an electron and a hole are trapped on the same site, they form a localized exciton and radiative recombination occurs with a fast relaxation time. If this is not the case, the recombination occurs between different sites with a slow relaxation time. A longer distance between the sites results in slower relaxation time. This is one of the origins of the decay-time distribution. As the carrier density increases, the probability of excited electron and hole pairs at the same site or in nearby sites increases, which means that radiative recombination time $\tau_{radiative}$ decreases. Since the non-radiative centers are already filled up in this density region, the decrease in τ_m directly means a decrease in $\tau_{radiative}$. The decrease of $\tau_{radiative}$ also causes an increase of the PL efficiency. Actually, the PL intensity gradually increases below N_{peak}, but the decrease of τ_m continues above N_{peak}. This may be caused by other non-radiative processes (outside the localized state, Auger effect, and so on). The mechanism of such non-radiative process is still an open question.

4. Summary

We have investigated the photo-generated carrier dynamics of InGaN/GaN nanocolumns. We used two samples, one containing InGaN/GaN MQW nanocolumns and a thin film for reference. We measured PL and TRPL spectra at liquid nitrogen temperature and fitted the TRPL data with a stretched exponential function. We were able to explain the carrier-density dependences of the PL spectrum, PL efficiency and average relaxation time τ_m by considering the filling of non-radiative centers, emission from localized states, processes at densities above the mobility edge density and other non-radiative processes. We have also showed the nanocolumns have high luminous efficiency even in the orange and red regions.

Acknowledgements

This work was supported by JSPS KAKENHI Grant Numbers 25800180, 24000013.

References

[1] M. Yoshizawa, A. Kikuchi, M. Mori, N. Fujita and K. Kishino, 1997. Growth of Self-Organized GaN Nanostructures on Al_2O_3 (0001) by RF-Radical Source Molecular Beam Epitaxy. Jpn. J. Appl. Phys. 36 L459.

[2] A. Kikuchi, K. Yamano, M. Tada and K. Kishino, 2004. Stimulated emission from GaN nanocolumns. Phys. Stat. Sol. (b) 241, No. 12.

[3] H. Sekiguchi, K. Kishino and A. Kikuchi, 2010. Emission color control from blue to red with nanocolumn diameter of InGaN/GaN nanocolumn arrays grown on same substrate. Appl. Phys. Lett. 96, 231104.

[4] K. Kishino, H. Sekiguchi, and A. Kikuchi, 2009. Improved Ti-mask selective-area growth (SAG) by rf-plasma-assisted molecular beam epitaxy demonstrating extremely uniform GaN nanocolumn arrays. Journal of Crystal Growth 311, 2063–2068.

[5] C. P. Lindsey and G. D. Patterson, 1980. Detailed comparison of the Williams–Watts and Cole–Davidson functions. J. Chem. Phys. 73, 3348.

[6] M.N. Berberan-Santos, E.N. Bodunov and B. Valeur, 2005. Mathematical functions for the analysis of luminescence decays with underlying distributions 1. Kohlrausch decay function (stretched exponential). Chemical Physics 315, 171–182.

[7] J. Naka, Y. Inose, H. Kunugita, K. Ema, V. Ramesh, A. Kikuchi and K. Kishino, 2012. Optical properties of InGaN/GaN nanocolumns in yellow-to-red region. Phys. Status Solidi C 9, No. 12.

[8] S. F. Chichibu, T. Azuhata, H. Okumura, A. Tackeuchi, T. Sota and T. Mukai, 2002. Localized exciton dynamics in InGaN quantum well structures. Applied Surface Science 190, 330–338.